Robotica (2023), **41**, pp. 1762–1777
doi:10.1017/S0263574723000139

CAMBRIDGE UNIVERSITY PRESS

RESEARCH ARTICLE

Research on effects of different internal structures on the grasping performance of Fin Ray soft grippers

Jiaqiang Yao, Yuefa Fang* and Luquan Li

School of Mechanical, Electronic and Control Engineering, Beijing Jiaotong University, Beijing, PR China, 100044
*Corresponding author. E-mail: yffang@bjtu.edu.cn

Received: 24 May 2022; **Revised:** 29 October 2022; **Accepted:** 10 January 2023; **First published online:** 15 February 2023

Keywords: soft robotics, soft robotic gripper, adaptive grasping, Fin Ray structure, finite element analysis

Abstract
Fin Ray soft grippers, as a notable passive compliant structures, can be easily actuated by external devices to adapt their shape to conform to a grasped object. Their unique ability is aided by their V-shaped structure and morphable material utilized by the Fin Ray finger. Thus, when the internal structure changes, the adaptability and grasping abilities also change. However, related works focus on the effects of changing key parameters on the grasping performance based on the Festo structure, and few works have explored the effects of changing the internal structure. To close the research gap, four different Fin Ray structures are presented in this article, and a parameter determination process was carried out by maximizing their adaptability by investigating the key parameters of each structure through finite element analysis. Then, the force responses of four selected Fin Ray structures are analyzed and experimentally validated. The results show that the No Internal Filling structure obtained by omitting the crossbeams is ideal for grasping delicate targets with the best adaptability and the minimum resultant force. The cross structure attained by adding vertical beams connected to crossbeams decreases the adaptability of the Fin Ray finger but significantly increases the contact force. The unsymmetric design of the branched structure significantly enhances the final contact force while improving the passive adaptation to objects. Thus, the application of the Fin Ray finger ranges from adaptive delicate grasping tasks to high-force manipulation tasks.

1. Introduction

Soft robot grippers (SRGs), as good examples of soft robot technologies, are generally composed of soft [1, 2], flexible, and compliant materials that conform to the shape of an object so that the gripper will grasp objects of various sizes and shapes without causing damage. SRGs have been widely utilized in robotic grasping and manipulation applications, such as the pick-and-placement of difficult-to-handle and delicate objects, including raw eggs [3–6], light bulbs [7, 8], flexible textiles [9, 10], and various food items [11–13]. Compared with conventional rigid robots, which are typically designed to perform precise and accurate tasks under advanced control systems using sensors to provide feedback [7], SRGs are usually actuated to conform to objects because of their intrinsic soft and morphable materials and structures. Additionally, compared with the point contact and finite plane contact of conventional rigid/hard grippers, soft grippers can have infinite degrees of freedom that exhibit continuous deformations when interacting with objects. Fin Ray fingers, as one of the most famous examples of passive compliant structures, can be easily actuated by external devices that are independent of the main structures and have a wide range of selection, which renders the design, fabrication, and implementation of such SRGs practical and convenient [14]. The Fin Ray finger is inspired by the deformation of fish fins and was invented in 1997 by Leif Kniese [15]. The Fin Ray effect (FRE) is a counterintuitive reaction that, when a compressive load is applied, does not bend away from the load but instead bends in the direction of the load. Biologically, this structure is composed of two bones in the shape of a V linked by connective tissue. This particular design, when realized by flexible materials, allows the finger to adapt its shape to conform to a grasped object, allowing simple yet reliable manipulation.

Since the Fin Ray finger was first utilized in the Bionic Tripod as an adaptive gripping finger by the company Festo [16], several subsequent studies on Fin Ray structures have already been conducted. These related studies mainly focus on two aspects: modeling of the Fin Ray finger and optimization of the structure. To predict the deformation shape and force of the Fin Ray soft gripper contacting an object, the kinetostatic models of the multicross beams of the Fin Ray finger were separately established by Shan [17] and Costanza Armanini [18] using an improved pseudo-rigid body model and extended discrete Cosserat approach. Others focus on the improvement in the grasping performance of Fin Ray fingers by structural optimization. For example, Khaled Elgeneidy [19, 20] discovered an increasing number of crossbeams and tilted them towards the contact surface. A layer jamming effect can be easily caused when the Fin Ray finger is pressed against an object. In this jammed state, the overall stiffness of the Fin Ray finger increases, causing a significant increase in the gradient of the force response. Loong Yi Lee [21] used a spring to exert a grasping force on objects based on the Festo structure and investigated the grasp force and dynamic reaction force exerted upwards during grasping with different incline angles of the crossbeam towards the Fin Ray finger base. Ivan Basson [22, 23] investigated the impacts of changing the geometry of ribs on the performance of Fin Ray finger; the FEA simulation results revealed that designing Fin Ray fingers with circular curved sloped ribs enhance the mass holding ability and conformity performance for the finger. A Fin Ray finger constructed from hard and soft materials was created by Crooks *et al.* [24], and models in FEA showed that the new Fin Ray finger can deform 15% more than traditional Fin Ray fingers when subjected to the same force. Notably, in the modeling process of the two accurate mathematical models of the Fin Ray mechanism, the crossbeams were modeled as being connected with the front and back beams by revolute joints or were just designed as rigid. The deformation of the crossbeams was limited to simplifying the modeling process. However, this simplification also influences the researcher's concentration on the various designs of internal structures and their influence on grasping performance. Compared with the Fin Ray fingers with rigid ribs, the benefits of integrated design with soft materials include having no sliding parts (and therefore no friction or stick-slip effects), having no backlash, and simplifying the fabrication process. Moreover, these benefits offer more possibilities to improve the grasping performance of the Fin Ray finger by changing its internal structure and optimizing the parameters of the structure. However, among all these studies, few works have analyzed the effects of different internal structures on the grasping performance of soft grippers. The potential of improving the grasping performance of Fin Ray fingers with various designed internal structures is limited.

In this article, we focus on the effects of different internal structures on the grasping performance of Fin Ray soft grippers. Four different Fin Ray structures with their parametrical model are proposed: the Festo structure, No Internal Filling structure, Branched structure, and Cross structure. The research process is divided into two steps. First, the parameter determination process was carried out by investigating the effects of different parameter values on the adaptability of each Fin Ray structure. Then, four Fin Ray structures with the best adaptability within the given ranges of parameter values are obtained. Second, the adaptability and grasping force of four selected Fin Ray structures are compared, and the effects of different internal structures are analyzed. The work in this article may facilitate the inspiration and development of future Fin Ray soft grippers with an increase in the number of functional structures.

The remainder of this article is organized as follows: Section 2 describes the research process and the method used to evaluate the structure with the best adaptability. Additionally, four different Fin Ray structures and their parametric models are designed. Then, details about the conducted finite element analysis (FEA) are presented in Section 3, outlining each parameter determination process. Furthermore, the FEA results are presented, starting with the effects of different design parameters on each structure's adaptability, followed by the adoption of the selected parametric model with the best adaptability of each structure. Then, the adaptability and force response of different selected Fin Ray structures are compared and evaluated, simultaneously introducing the advantages and disadvantages of each Fin Ray structure. The four selected Fin Ray fingers were experimentally tested to validate the FEA results in Section 4. Section 5 concludes this article and outline plans for future work.

2. Research process description and parametric Fin-Ray structure design

2.1. Fin Ray soft grippers with different internal structures

In related research [18, 20, 25], researchers have shown that the increment improvement of the Festo finger design can be achieved by parameter determination based on FEA. However, the structure of the soft crossbeams varies, which changes the distribution of the stiffness of the Fin Ray soft grippers. To explore the influence of different internal structures of the Fin Ray soft grippers on the grasping performance, four Fin Ray fingers with particular internal structures are proposed and their parametric models are established, which will be detailed in the next subsection. Then, the parameter determination process needs to be implemented on the four Fin Ray structures to improve their adaptability.

Among the past related works, different evaluation criteria were applied for the parameter determination. For the Fin Ray finger with rigid crossbeams, the maximum displacement of the Fin Ray finger caused by the same point force under different parameters is selected as the indication to improve the adaptability of the Fin Ray finger by Rui Chen *et al*. [25]. The greater arch-like shape structure when increasing the point force on the same height of the contact beam is selected as the optimal structure [18]. For structures with soft crossbeams, tip displacements are always used to evaluate the compliance ability of the Fin Ray fingers, such as the total tip displacements [24], the tip displacements along two axes of the bending plane [20], the combination of tip displacement, and finger displacement at the contact point [6]. Among these evaluation criteria, we discovered that the method of analyzing tip displacements along two axes of the bending plane is more general since different Fin Ray fingers can have different tip displacement behaviors corresponding to their bases. These behaviors are investigated in the next section by developing accurate finite element models of the soft FRE fingers that effectively capture its deformation behavior so that a range of structural variations can be simulated and evaluated in terms of improvement in adaptability when grasping objects. Overall, the research process is divided into two steps:

1. First, parametric models of four Fin Ray structures are established. Second, tip displacement along two axes serves as an indication to evaluate the adaptability of the Fin Ray structure to achieve parameter determination. Last, based on FEA, four Fin Ray structures with the best adaptability within the ranges of parameter variables are obtained.
2. The adaptability and grasping force of the four selected Fin Ray structures are compared and the effects of different internal structures on grasping performance are summarized.

2.2. Parametric Fin Ray structure design

The dimensions of the finger, including the thickness of the front and back beams, the height of the FRE fingers (H), and the width of the FRE fingers (W_1 and W_2) were unified. According to existing research [25], a structure with a higher stiffness of the back beam will have a higher percentage of positive contact forces, which makes it easier for the finger to not only compliantly and tightly conform to an object surface, but also to simultaneously minimize lateral deformation. Therefore, for all analyzed Fin Ray structures, the thickness of the front beam was set to 1 mm, and that of the back beam was set to 2 mm. Here, we refer to the beam that touches the object as the front beam and refer to the other side as the back beam. Additionally, the shape of two longitudinal beams was designed as a trapezoid, which showed a better grasping ability, with a fixed height $H = 100$ mm, bottom width $W_1 = 32$ mm, and top width $W_2 = 16$ mm taking into account the dimensions of regular objects, as shown in Fig. 1.

To further analyze the effects of different internal structures on the grasping performance of Fin Ray fingers, four different internal structures and their parametric models, as shown in Fig. 2, were developed. Four particular internal structures were proposed for the following reasons:

1. The Festo design was retained in our work to make a performance comparison with the newly proposed Fin Ray structures.

https://doi.org/10.1017/S0263574723000139 Published online by Cambridge University Press

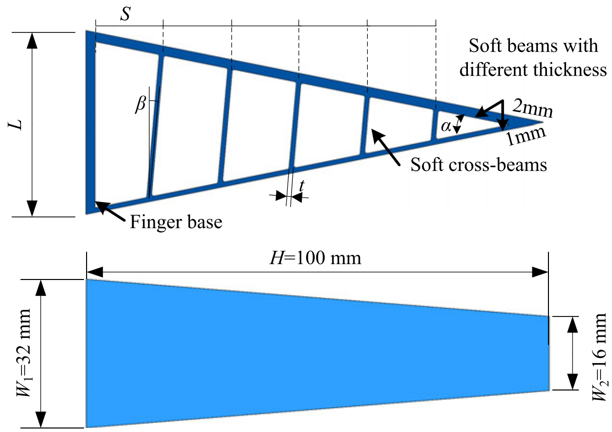

Figure 1. *Parametric model of the Fin Ray finger with relative dimensions.*

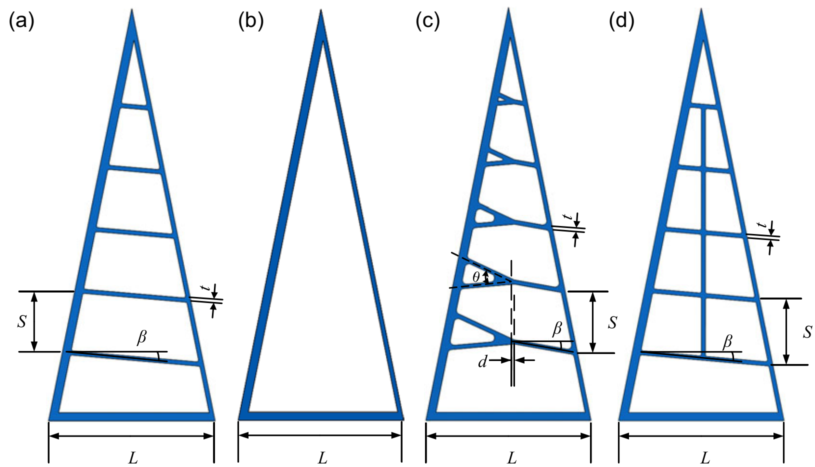

Figure 2. *Crossbeam structure: (a) Festo structure, (b) No Internal filling structure, (c) Branched structure, and (d) Cross structure.*

2. The natural individual fin rays are composed of two half-ray elements (referred to as hemitrichs) connected by collagen fibrils and covered with skin [26, 27]. There is no apparent crossbeam structure between the two vertical beams. Thus, the No Internal Filling structure was proposed to analyze the influence on the grasping performance.
3. The existing Fin Ray fingers are designed with symmetrical crossbeams. The branched structure can inspire unsymmetrical Fin Ray structures designed to further improve the grasping performance.
4. In past Fin Ray fingers, the crossbeams were designed so that they did not to interconnect. However, in natural fin rays, the collagen fibrils are sandwiched between two stiff beams (hemitrichs) along the ray [26]. The Cross structure was proposed to analyze the influence on the grasping performance by connecting different crossbeams.

Notably, Fin Ray finger designs are not restricted to the four kinds of internal structures proposed in our work. Any structure that can act as a virtual flexural hinge at the connection with vertical beams can be considered an option to design the new Fin Ray finger.

Table I. *Range of values of each tested parameter of Fin Ray fingers.*

Parameter	Symbol	Range	Increment
Equal spacing between each crossbeam	S	$12 \sim 18$ mm	2 mm
Thickness of crossbeams	t	$0.6 \sim 1.2$ mm	0.2 mm
Length of the finger base	L	$30 \sim 60$mm	10 mm
Incline angle of the crossbeam	β	$-10 \sim 10^\circ$	5°
Angle of two-branched ribs	θ	$20 \sim 50^\circ$	10°
Distance of two-branched ribs shifting from the central axis	d	$-2 \sim 1$ mm	1 mm

The parametric model was developed for the proposed Fin Ray structures. For the Festo structure and Cross structure, three parameters–open angle α of the finger bottom, equal spacing S between each crossbeam, thickness t of the crossbeams, and incline angle β of the crossbeam towards the finger base–were determined. For the No Internal Filling structure, only the parameter of the open angle α of the finger bottom was considered. The parametric model of the branched structure, including the open angle α of the finger bottom, the equal spacing S between each crossbeam, the thickness t of the crossbeams, the angle θ of the two-branched ribs, the incline angle β of the crossbeam towards the finger base, and the distance d of the two-branched ribs shifting from the central axis of the finger, was more complicated. In addition, the positive and negative distances determined whether the branched ribs shifted to the right side or to the left side. For all structures, since the dimensions were determined, the open angle α could be adjusted by changing the length L of the finger base. Note that the smaller the spacing S is, the greater the number of crossbeams that will be included. Additionally, when the value of the incline angle becomes negative, the crossbeams are tilted towards the grasped object.

3. The performance comparison and parameter determination based on FEA

3.1. FEA

A static structural analysis for the deformation of the Fin Ray soft grippers was created using ANSYS software. Since the FRE was discovered and proposed, different materials have been attempted for use in Fin Ray fingerprinting, such as NinjaFlexC [19, 20, 28], ABS [18, 29, 30], thermoplastic polyurethane (TPU) [14, 21, 31, 32], and mixed rubber silicone [25]. For a Fin Ray finger with mixed material, material casting or mould processes are always utilized. The other three kinds of material fingers can be fully 3D printed. Fin Ray fingers constructed of different materials exhibit variable stiffness, flexibility, friction, or elasticity. The Acrylonitrile Butadiene Styrene (ABS) material with high elastic modulus was selected for the side beams in the Fin Ray finger with rigid crossbeams [18]; steel rings were used as crossbeams in this finger placed inside the designated holes of the side beams; and the special design allowed movement between the side beams and the crossbeams. However, for Fin Ray fingers with soft crossbeams, the movement between the side beams and the crossbeams relies on the deformation of soft and morphable cross-beams. Thus, the softer material is selected as the first choice to fabricate the integrated Fin Ray soft gripper. To the best of the author's knowledges, Ninjaflex does not appear as a standard material within the ANSYS package [33]. TPU has a maximum recoverable strain of 50% and Young's modulus ranging from 10 to 1000 MPa, which is much softer than ABS plastic. In this article, the material we used in Fin Ray soft grippers is TPU 95A with a Young's modulus of 26 MPa and Poisson's ratio of 0.48. For ease of analysis, it is assumed that the finger only has isotropic material properties from a combination of multiple 3D-printed layers in different directions. As described in Section 2.1, four different Fin Ray structures should be optimized with the aim of maximizing the adaptability. This article follows the previous method of parameter determination to incrementally improve the adaptability of the gripper. Four different Fin Ray structures were parameterized on ANSYS to simulate the deformation of the fingers at a range of values for each tested parameter given in Table I.

https://doi.org/10.1017/S0263574723000139 Published online by Cambridge University Press

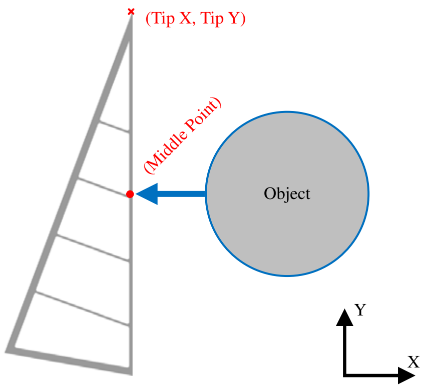

Figure 3. *Illustration of the FEA study showing the spherical object and Fin Ray soft gripper.*

Each parameter determination process is divided into several steps as follows:

Step 1: For each tested parametric model, the front beam of the Fin Ray finger was set to be perpendicular to the grasped object at the beginning with the object loaded at the same height as the finger base, approximately at the middle point of the front beam where the largest deformation would occur as highlighted in Fig. 3.

Step 2: The material of the Fin Ray finger was designated as TPU 95A and the object was treated as a rigid body. The contact status between the finger and the object was defined according to a frictional relationship, and the frictional coefficient was defined as 0.24. In addition, the finger was fixed at its base to simulate a rigid connection to the actuator and the object was constrained to move only along the X-axis.

Step 3: A circular object with a diameter of 20 mm was simulated to translate a total of 20 mm with a step of 1 mm against the simulated Fin Ray soft gripper. After each simulation, the resulting tip displacement along two axes in the plane as the object presses against the finger and causes the flexible structure to deform and adapt was recorded.

For each tested parameter, at least four simulations from step 1 to step 3 need to be implemented to determine the best parameter value within the given range in Table I.

3.2. FEA results

3.2.1. Passive adaptation

Different simulations were carried out with the parameter determination process described in Section 3.1. In this section, the effects of different parameters of the Fin Ray structure on the tip deflection were evaluated to highlight the enhancement of passive adaptation. Four Fin Ray soft grippers with different internal structures were selected with the best adaptability within the given range values.

The first improved internal structure for the Fin Ray soft gripper was the Festo structure shown in Fig. 2(a). For this structure, four different parameters–spacing, crossbeam thickness, base length, and incline angle–were evaluated. Four different spacings ($S = 12$, 14, 16, and 18 mm), four different thicknesses ($t = 0.6$, 0.8, 1.0, and 1.2 mm), four different base lengths ($L = 30$, 40, 50, and 60 mm), and four different incline angles ($\beta = -10^\circ$, -5°, 5° and 10°) were selected as the determination variables. For the first simulation with regard to the different spacings, the model with a thickness of 1 mm, length of 40 mm and incline angle of 0° was employed.

Figure 4 shows the recorded X and Y tip displacements of each of the tested parameter values against the 20 mm displacement of the object pushing the Fin Ray fingers. The object is displaced only along the negative X-axis direction. For the variation in spacing, Fig. 4(a) shows that the tip of the structure with a 16 mm spacing has moved 3.44 mm along the X-axis at the end of the 20 mm displacement imposed

https://doi.org/10.1017/S0263574723000139 Published online by Cambridge University Press

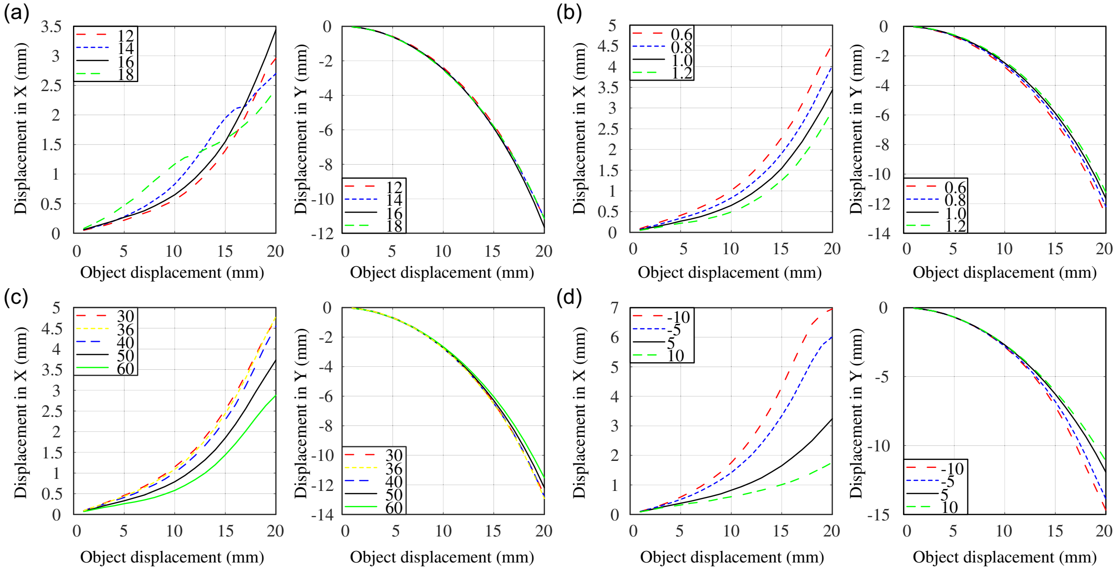

Figure 4. *Effects of varying the parameters of the Festo structure on the tip displacement along the X- and Y-axes. (a) spacing, (b) thickness, (c) base length, and (d) incline angle.*

by the object, compared with only a 2.44-mm tip displacement by the 18 mm spacing structure. It is generally observed that the fingertips are pushed along the opposite direction of object displacement, yet the structure with more tip travel in the X-axis means better adaptation since the object displacement is being absorbed by the Fin Ray soft gripper. Similarly, the 16-mm spacing structure moved 11.65 mm towards the object along the Y-axis, compared with 11.16 mm displacement by the 18 mm spacing structure. In this case, more travel along the Y-axis is desired, as it means that the tip is closing on the object pushing the Fin Ray finger along the X-axis. Although the tip displacement does not manifest a monotonic tendency as the spacing value increases, the chosen four values of spacings corresponding to the numbers of crossbeams of the Fin Ray finger varied from 3 to 6. In addition, the tip displacement of the 16 mm spacing structure manifests the best coherence as the object displacement increases as shown in Fig. 4(a). Hence, a finger structure with a spacing of 16 mm (while the number of crossbeams was 4) was adopted. Based on this approach, Fig. 4(b) shows that the tip displacement monotonically decreases at the end of the 20 mm displacement imposed by the object as the thickness of the crossbeams varies from 0.6 mm to 1.2 mm in increments of 0.2 mm. Therefore, a thickness of 0.6 mm was adopted. For Fig. 4(c), the tip displacement along the X-axis monotonically decreases at the end of the 20 mm displacement imposed by the object as the length of the finger base (related to the open angle) increases with 4 crossbeams spaced. However, the Y tip displacement of the 30 mm base length structure is smaller than that of the 40 mm base length structure, then decreases as the length of the finger base increases. Hence, four more lengths of finger base varying from 30 mm to 40 mm in increments of 2 mm (between which only the length structure with the best compliance is shown in Fig. 4(c)) were utilized to explore this relationship. The final adopted structure with a 36 mm length of the finger base moved 4.78 mm along the X-axis and 12.92 mm along the Y-axis. As shown in Fig. 4(d), when the incline angle of the crossbeams becomes positive, the maximum tip displacement monotonically decreases as the incline angle increases. However, when the incline angle of the crossbeams becomes negative, increasing the incline angle benefits the shape adaptation of the Fin Ray soft gripper, as the fingertip can close further on a target object. Therefore, the incline angle of -10° of the crossbeams was adopted, as a larger angle may lead to structural interference. Based on the above analysis, 16 mm, 0.6 mm, 36 mm, and -10° as the spacing between each crossbeam, crossbeam thickness, finger base length, and crossbeam incline angle, respectively, were adopted as the best parameters of the Festo structure Fin Ray finger.

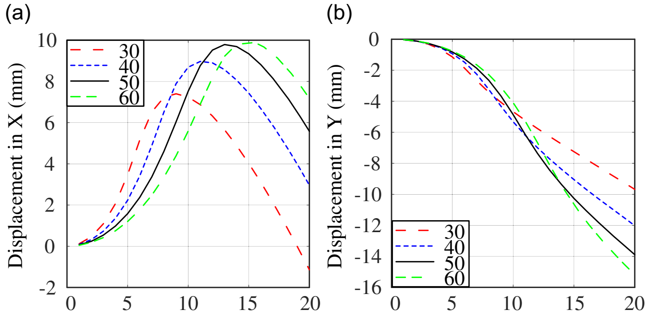

Figure 5. *Effects of varying the base length of the No Internal Filling structure on the tip displacement along the X- and Y-axes.*

The second evaluated internal structure was the No Internal Filling Fin Ray structure, as shown in Fig. 2(b). For this structure, only the finger base length was evaluated. Figure 5 shows the recorded X and Y tip displacements of the tested parameter with four different values ($L = 30$, 40, 50, and 60 mm) against the 20 mm displacement of the object pushing the Fin Ray fingers. Compared with the other three structures analyzed in this article, the No Internal Filling Fin Ray finger has the lowest stiffness owing to no interstructure support. Thus, using the same object pushing the Fin Ray finger, the No Internal Filling Fin Ray finger has the maximum tip displacement compared with the Fin Ray finger with internal structures. As shown in Fig. 5, the relationship of the tip displacement along the X-axis with the object displacement is different from that of the Festo Fin Ray finger. The tip displacement slowly increases to the peak value and then rapidly decreases to a small value (the 30 mm finger base length structure even has a negative tip displacement along the X-axis) as the object pushes the Fin Ray finger. The appearance of the inflection point reveals that at this moment the back beam of the structure is not sufficient to support the front beam to absorb the increasing grasp force by further bending. After this moment, the Fin Ray finger will keep its bending state basically unchanged, and the entire finger passively deforms under the external force from the object. In addition, Fig. 5 shows that the tip displacement monotonically increases at the end of the 20 mm displacement imposed by the object as the length of the finger base varies from 30 mm to 60 mm in increments of 10 mm. Increasing the length of the finger base results in a strengthening of the Fin Ray base, which dramatically increases the stiffness of the Fin Ray finger under loading [34]. As a result, the structure can support the Fin Ray finger bending more towards the object before the back beam cannot support the front beam deformation in the positive direction. Based on the above analysis, the base length of 60 mm was adopted as the best parameter of the No Internal Filling structure Fin Ray finger.

The third improved internal structure for the Fin Ray soft gripper was the Branched structure shown in Fig. 2(c). Based on the Festo structure, the Branched structure revises the geometry of the cross-beams, changing it to a structure with two ribs connected to the back beam and one rib connected to the front beam. This unsymmetric structure theoretically provides greater support to the front beam to improve the adaptability and final contact force of the Fin Ray finger. For this structure, six different parameters were evaluated, including spacing, crossbeam thickness, finger base length, incline angle, angle of two-branched ribs, and distance of the two-branched ribs shifting from the central axis. Four different spacings ($S = 12$, 14, 16, and 18 mm), four different thicknesses ($t = 0.6$, 0.8, 1.0, and 1.2 mm), four different lengths ($L = 30$, 40, 50, and 60 mm), four different incline angles ($\beta = -10^\circ$, -5°, 5° and 10°), four different angles of the two-branched ribs ($\theta = 20^\circ$, 30°, 40° and 50°), and four different distances of the two-branched ribs shifting from the central axis ($d = -2$, -1, 0, and 1) were selected as the determination variables. For the first simulation with regard to the different spacings, the model with the thickness of 1 mm, length of 40 mm, incline angle of 0°, angle of the two-branched ribs of 30°, and distance of the two-branched ribs shifting from the central axis of 0 was employed.

https://doi.org/10.1017/S0263574723000139 Published online by Cambridge University Press

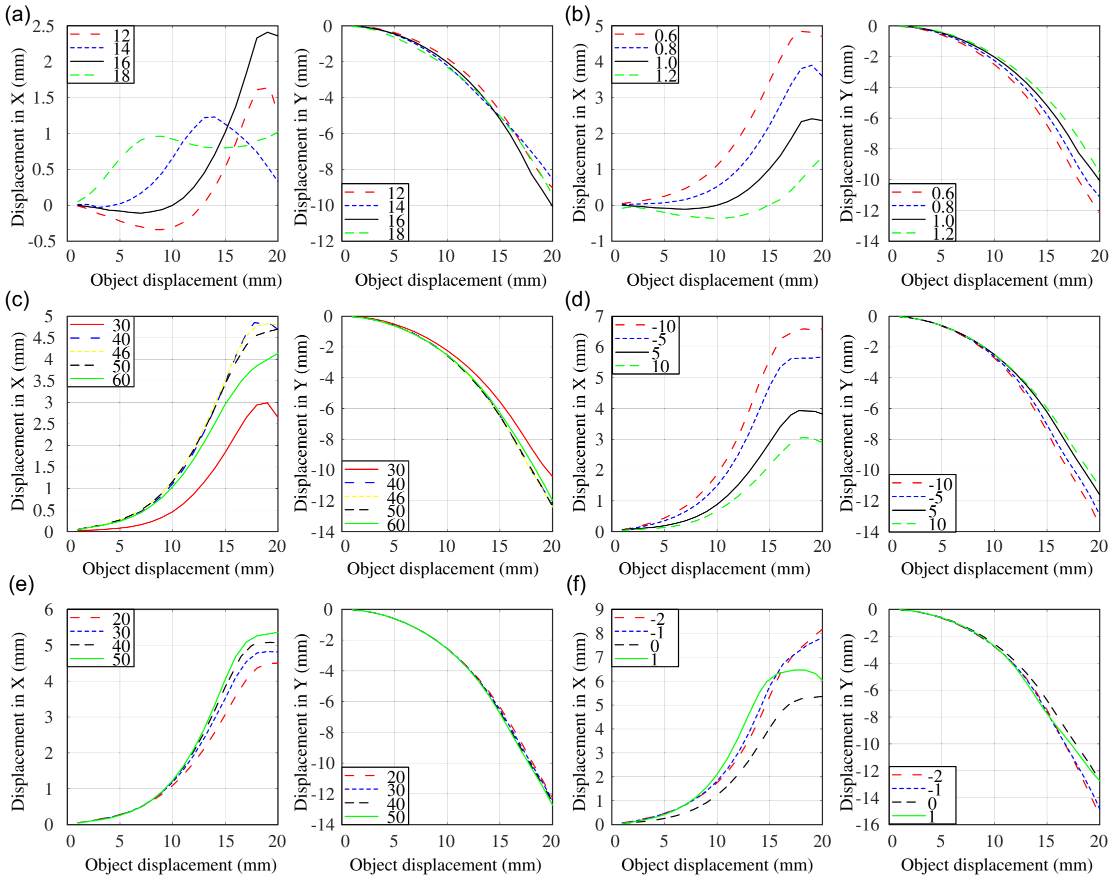

Figure 6. *Effects of varying the parameters of the Branched structure on the tip displacement along the X- and Y-axes. (a) spacing, (b) thickness, (c) base length, (d) incline angle, (e) angle of the two-branched ribs, and (f) distance of the two-branched ribs shifting from the central axis.*

Figure 6 shows the recorded X and Y tip displacements of each of the tested parameter values against the 20 mm displacement of the object pushing the Fin Ray fingers. For the variation of the spacing, Fig. 6(a) shows that at the end of the 20 mm displacement imposed by the object, the 16 mm structure has the maximum tip displacement along the X-axis and Y-axis which were 2.36 mm and 10.06 mm, respectively. Considering that the four chosen values of the spacings of the crossbeams corresponded to four different numbers of crossbeams, additional values were not chosen to optimize the spacing. Hence, a finger structure with a spacing of 16 mm (while the number of crossbeams was 4) was adopted. Notably, the adopted spacing value is equivalent to that of the Festo structure, but the tip displacement along the X-axis of the Branched Fin Ray finger does not monotonically increase as the object displacement increases. To acquire the desired structure with the tip displacement increasing as the object pushes the finger, the other five parameters were further evaluated to optimize the structure. As shown in Fig. 6(b) and (d), decreasing the thickness of the crossbeams and tilting the crossbeams towards the grasped object creates a preferred bending direction that can generally improve grasping performance. Therefore, a thickness of 0.6 mm and an incline angle of $-10\,^\circ$ were adopted. For Fig. 6(c), the tip displacement at the end of the 20 mm displacement imposed by the object increases and then decreases as the finger base length increases. The tip displacement of the 40 mm length structure and 50 mm length structure moved almost the same displacement along the X-axis and Y-axis. To further optimize the parameter of the finger base length from the range of the values, four additional values of finger base

https://doi.org/10.1017/S0263574723000139 Published online by Cambridge University Press

length ($L = 42$, 44, 46, and 48 mm) were evaluated to improve the adaptability of the Fin Ray finger. As shown in Fig. 6(c), the 46 mm length of the finger base was adopted with the largest displacement along the X-axis and Y-axis which were 4.81 mm and 12.40 mm, respectively. Figure 6(e) shows that the tip displacement monotonically increases at the end of the 20-mm displacement imposed by the object as the angle of the two-branched ribs increases. Hence, the angle of the two-branched ribs of 50 ° was adopted, as a larger angle may lead to structural interference. As shown in Fig. 6(f), the 0 mm shifting distance structure has the minimum tip displacement among the chosen values. When the shifting distance becomes positive, the Fin Ray finger has a slight improvement in compliance with the object. When the shifting distance becomes negative, the maximum displacement dramatically increases as the distance increases. Therefore, the distance of two-branched ribs shifting from the central axis of −2 mm was adopted. Based on the above analysis, 16 mm, 0.6 mm, 46 mm, −10 °, 50 °, and −2 as the spacing between each crossbeam, crossbeam thickness, finger base length, inclined angle, angle of the two-branched ribs, and distance of the two-branched ribs shifting from the central axis, respectively, were adopted as the best parameters of the Branched structure Fin Ray finger.

The last evaluated internal structure for the Fin Ray soft gripper was the Cross Fin Ray structure shown in Fig. 2(d). Based on the Festo structure, the Cross Fin Ray structure adds vertical beams to connect the crossbeams. The added vertical beams make the crossbeams correlate, decreasing the maximum deformation of the crossbeams. The overall stiffness of the Fin Ray finger is increased, causing a significant increase in the gradient of the force response. Since the geometry of the crossbeams is unchanged, the performance of the Cross and Festo structures in terms of passive adaptation and force response when grasping objects is theoretically similar. Therefore, four parameters equivalent to those of the Festo structure are evaluated: spacing, crossbeam thickness, base length, and incline angle. Four different spacings ($S = 12$, 14, 16, and 18 mm), four different thickness ($t = 0.6$, 0.8, 1.0, and 1.2 mm), four different lengths ($L = 30$, 40, 50, and 60 mm), and four different incline angles ($\beta = -10\,°$, $-5\,°$, $5\,°$ and $10\,°$) were selected as the determination variables. For the first simulation with regard to the different spacings, the model with a thickness of 1 mm, length of 40 mm and incline angle of 0 ° was selected.

Figure 7 shows the recorded X and Y tip displacements of each of the tested parameter values against the 20 mm displacement of the object pushing the Fin Ray fingers. Compared with the Festo structure, the four evaluated parameters manifest almost the same influence on the compliance of the Fin Ray finger. Hence, the detailed evaluation process of different parameters can refer to the Festo structure. The tip displacement of the final improved Branched structure Fin Ray finger moved 5.73 mm and 13.33 mm along the X-axis and Y-axis, respectively. The specific values of the selected parameters are 16 mm, 0.6 mm, 38 mm, and −10 ° as the spacing between each crossbeam, crossbeam thickness, finger base length, and incline angle of the crossbeams, respectively. As described in Section 2.1, the effects of the parameters of different structures are investigated and the parametric models of different structures with the best adaptability are selected. Then, the effects of different internal structures of the Fin Ray finger on the grasping performance are evaluated.

3.2.2. *Effects of different internal structures on grasping performance*

The effects of the parameters of different structures have been investigated and four Fin Ray fingers have been selected with the best adaptability in Section 3.2.1. In this section, the effects of different internal structures on grasping performance (which includes adaptability and force response of the Fin Ray finger) are evaluated.

Figure 8 compares the recorded X and Y tip displacements of four selected Fin Ray structures against the 20 mm displacement of the object pushing the fingers. The force responses from different structures are shown in Fig. 9. These two figures show that the selected No Internal Filling structure has the maximum tip displacement towards the grasped object while at the same time maintaining the minimum final contact force during the four different Fin Ray structures. This finding illustrates that the design of a Fin Ray finger without an internal structure decreases the overall stiffness of the Fin Ray finger,

https://doi.org/10.1017/S0263574723000139 Published online by Cambridge University Press

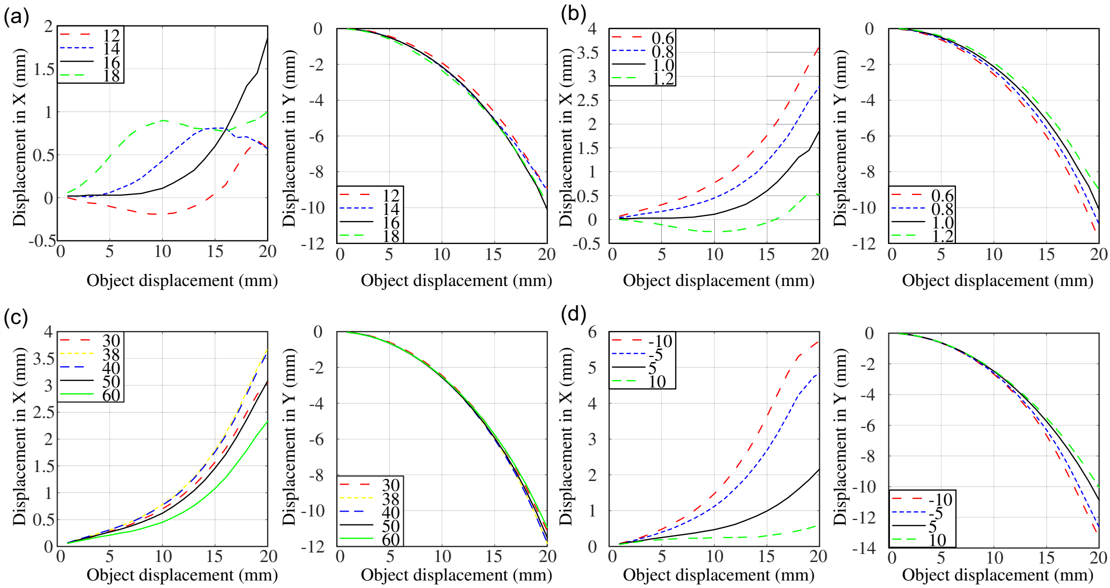

Figure 7. *Effects of varying the parameters of the Cross structure on the tip displacement along the X- and Y-axes. (a) spacing, (b) thickness, (c) base length, and (d) incline angle.*

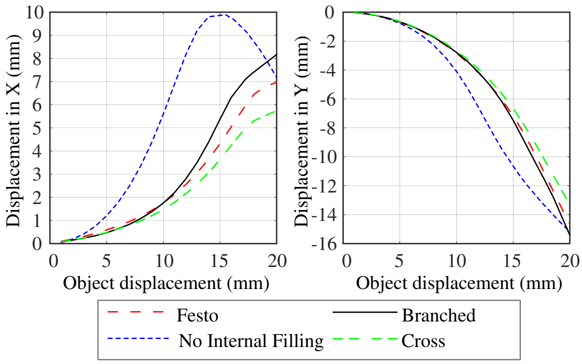

Figure 8. *Effects of different internal structures on the tip displacement along the X- and Y-axes.*

causing it to easily deform when interacting with an object, which is ideal for grasping delicate targets. In addition, note that the inflection point only happens in the relationship between tip displacement and object displacement for the No Internal Filling structure as at the moment the back beam of the structure is not sufficient to support the front beam to absorb the increasing contact force by further bending. This finding emphasizes the importance of the internal structure to the behavior of Fin Ray fingers throughout the grasping process. When the Fin Ray fingers are designed with soft and morphable internal structures, its overall stiffness of the finger will be increased, causing a significant increase in the final contact force, as shown in Fig. 9. Simultaneously, the tip displacement monotonically increases as the object pushes the finger. For the Cross structure, the added vertical beams make the crossbeams correlated, which decreases the adaptability of the Fin Ray finger but significantly increases the final contact force. Specifically, compared with the selected Festo structure, the selected Cross structure showed a reduction in the tip displacement towards the grasped object by 1.23 mm along the X-axis and 1.35 mm along the Y-axis, while simultaneously increasing the maximum contact forces by up to 31%. For the Branched structure with the asymmerical design of crossbeams, the adaptability of the Fin Ray finger improves

https://doi.org/10.1017/S0263574723000139 Published online by Cambridge University Press

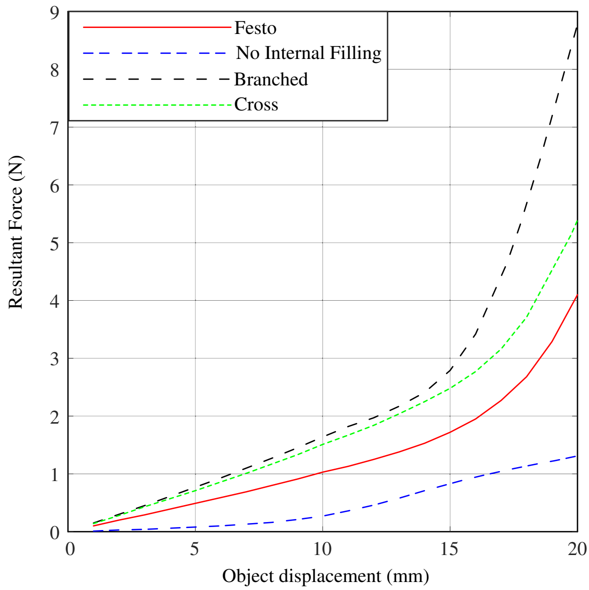

Figure 9. *Resultant force response after varying internal structures of Fin Ray fingers.*

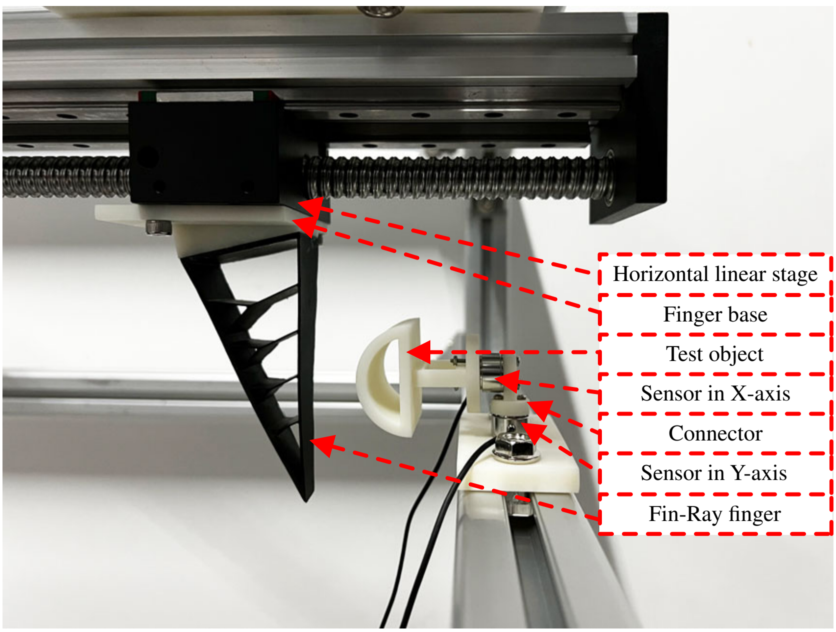

Figure 10. *Labelled experimental setup for testing Fin Ray soft gripper.*

and the force response dramatically increases compared with the Festo structure. Specifically, the maximum tip displacement towards the grasped object improved by 1.21 mm along the X-axis and 0.74 mm along the Y-axis, while simultaneously increasing the maximum contact forces by up to two times. This structure can broaden the applications of Fin Ray fingers to include not only delicate grasping but also high-force applications. Moreover, the work may facilitate the inspiration and development of future Fin Ray soft grippers with more functional structures.

https://doi.org/10.1017/S0263574723000139 Published online by Cambridge University Press

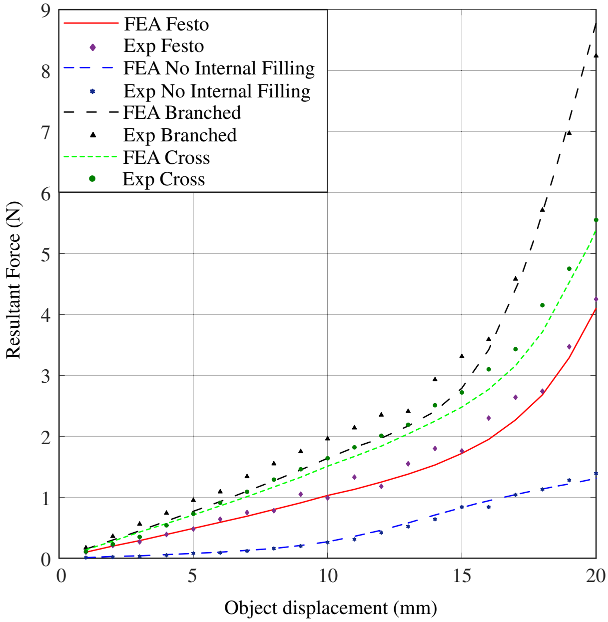

Figure 11. *Resultant force response (FEA vs. experimental) for four selected Fin Ray structures.*

4. Experiment validation

4.1. Experimental setup

To validate the FEA results, a test rig (shown in Fig. 10) was constructed to record the force response generated when testing four selected Fin Ray structures. The specific manufacturing process of a Fin Ray finger is described as follows: First, a rigid ABS model was 3D printed in the same shape as the selected Fin Ray structure. The model was surrounded by acrylic barriers to form a containment field. Second, a silicone rubber mixed per the recommendation was degassed and then slowly poured into the containment field until it was filled. The silicone rubber was then cured at room temperature for 24 h. Third, the silicone rubber was demould from the rigid model, and a new rubber mould was completed. Fourth, TPU 95 A with a hardness of 95° Shore A was slowly poured into the rubber model and then cured at room temperature for 6 h. Last, the Fin Ray structure was demould from the rubber mould and a Fin Ray finger was completed. A round target object was 3D printed from rigid ABS with the same diameter used in the simulation (20 mm). The sensor utilized in the experiment is the uniaxial compression tension sensor, which is provided by Simbatouch, China, and the model is SBT674-10. Each sensor has a measuring range of $0 \sim 10$ N and an accuracy of 0.01 N. To simultaneously measure the grasping force exerted on the object along the X-axis and Y-axis, a connector was designed to connect these two sensors as shown in Fig. 10. A motor-controlled horizontal linear stage displaces the Fin Ray soft gripper against the test object by a 20-mm stroke in 1 mm steps. At each step, the generated forces from the two uniaxial sensors are logged, and the resultant forces are calculated and compared with the corresponding data from FEA. The tested Fin Ray finger is fixed on the horizontal stage using a 3D-printed finger base. Four Fin Ray structures with the best adaptability according to the performance comparison and parameter determination based on FEA were fabricated and experimentally tested. Note that the experiment is repeated three times for each Fin Ray structure, and the average value is applied to reduce errors.

4.2. Experimental validation results

Figure 11 compares the force response from the FEA and mean experimental data for the four selected Fin Ray structures. The FEA results closely matched the experimental data from the physical tests,

https://doi.org/10.1017/S0263574723000139 Published online by Cambridge University Press

which confirms the accuracy of the FEA results. The experimental results were determined to be highly repeatable for the same structure. The maximum standard deviation for the four Fin Ray structures in the final resultant force was 0.058. The deviation is conjectured to mainly derive from the linear elastic material model in FEA. In our work, Young's modulus is the most important property of the material to compare the grasping force from the FEA with the experimental results. Since the different designs are being exclusively compared by their geometries, the material model in the FEA will not affect the research results.

5. Conclusions and future work

In this article, we focus on the effects of different internal structures on the grasping performance of Fin Ray soft grippers. Four Fin Ray fingers with different internal structures, including the No Internal Filling structure, Branched structure and Cross structure, are proposed. Then, the parametric model of each Fin Ray structure is established and the range of each parameter is given. To incrementally improve the adaptability of each Fin Ray structure, the tip displacement along two axes of the bending plane is selected as the indication to achieve the parameter determination process. Based on FEA, four Fin Ray structures with incremental improvements in adaptability are selected. Then, the adaptability and resultant force of four selected Fin Ray structures are compared and evaluated. The FEA results show that the selected Fin Ray structure without an internal structure has the best adaptability and minimum resultant force among the four Fin Ray structures. This finding illustrates that the design of a Fin Ray finger without an internal structure decreases the overall stiffness of the Fin Ray finger, causing the finger to easily deform when interacting with an object, which is ideal for grasping delicate targets. However, as the contact force increases, the adaptability of this kind of finger decreases as the back beam of the structure is not sufficient to support the front beam to absorb the increasing contact force by further bending. This finding emphasizes the importance of the internal structure to the behavior of Fin Ray fingers throughout the grasping process. When Fin Ray fingers are designed with soft and morphable internal structures, the overall stiffness of the finger increases, causing a significant increase in the final contact force. Simultaneously, the tip will deform towards the grasped objects when the object pushes the finger. For the Cross structure, the added vertical beams make crossbeams correlated when deformation occurs, which decreases the adaptability of the Fin Ray finger but significantly increases the final contact force. For the Branched structure with the asymmetrical design of crossbeams, the adaptability of the Fin Ray finger improved and the force response dramatically increased compared with the Festo structure. Specifically, the maximum tip displacement towards the grasped object improved by 1.21 mm along the X-axis and 0.74 mm along the Y-axis while simultaneously increasing the maximum contact forces by up to two times. The FEA results were experimentally validated and tested with four selected Fin Ray structures. The force response recorded from the experiment matched the simulation results across different samples, which confirms the accuracy of the FEA results.

This article is the first step to explore the effects of different internal structures on the grasping performance of Fin Ray soft grippers. The next stage of this work will involve the design of additional internal structures and investigate further structural and topological optimizations that enhance the grasping performance of grippers based on the work that we have achieved. A more interesting material model will be considered in future work to reduce the deviations between the experimental results and the simulation results. More evaluated indications will be considered in future work, such as the indication that qualifies how balanced the contact forces are, the ratio of the sum of the contact forces, and the actuation force at the base of the Fin Ray finger. The newly added indication can help guide researchers to creative Fin Ray fingers with different applications. For example, the cellular compliant mechanism can be considered as a new internal structure to empower the finger to grasp targets with a uniform contact force, which can greatly reduce damage to the grasped object due to concentrated stress.

Acknowledgment. The authors gratefully acknowledge the financial support from the National Natural Science Foundation of China Grant under grant number 51975039.

Author contributions. The work presented in this article was carried out under the supervision of Prof. Yuefa Fang of the School of Mechanical, Electronic and Control Engineering, University of Beijing Jiaotong. In addition, Dr. Luquan Li gave valuable suggestions and assisted with analyses.

Financial support. A research grant from the National Natural Science Foundation of China Grant under grant number 51975039.

Conflicts of interest. The authors declare none.

Ethical approval. None.

References

[1] J. Hughes, U. Culha, F. Giardina, F. Guenther, F. Rosendo, A. Rosendo and F. lida, "Soft manipulators and grippers: A review," *Front. Robot. AI* **3**, 69 (2016).
[2] R. Bogue, "Flexible and soft robotic grippers: The key to new markets?," *Ind. Robot Int. J*. **43**(3), 258–263 (2016).
[3] F. Ilievski, A. D. Mazzeo, R. F. Shepherd, Xin. Chen and G. M.Whitesides, "Soft robotics for chemists," *Angew. Chem*. **123**(8), 1930–1935 (2011).
[4] J. Shintake, S. Rosset, B. Schubert, D. Floreano and H. Shea, "Versatile soft grippers with intrinsic electroadhesion based on multifunctional polymer actuators," *Adv. Mater.* **28**(2), 231–238 (2016).
[5] W. Wang and S. H. Ahn, "Shape memory alloy-based soft gripper with variable stiffness for compliant and effective grasping," *Soft Robot.* **4**(4), 379–389 (2017).
[6] J. Suder, Z. Bobovský, J. Mlotek, M. Vocetka, P. Oščádal and Z. Zeman, "Structural optimization method of a FinRay finger for the best wrapping of object," *Appl. Sci*. **11**(9), 3858 (2021).
[7] H. I. Kim, M. W. Han, S. H. Song and S. H. Ahn, "Soft Morphing Hand Driven by SMA Tendon Wire," **In:** *Composites Part B: Engineering, vol. 105* (2016) pp. 138–148.
[8] J. R. Amend, E. Brown, N. Rodenberg, H. M. Jaeger and H. Lipson, "A positive pressure universal gripper based on the jamming of granular material," *IEEE Trans. Robot.* **28**(2), 341–350 (2012).
[9] J. Guo, K. Elgeneidy, C. Xiang, N. Lohse, L. Justham and J. Rossiter, "Soft pneumatic grippers embedded with stretchable electroadhesion," *Smart Mater. Struct*. **27**(5), 055006 (2018).
[10] J. Guo, C. Xiang and J. Rossiter, "A soft and shape-adaptive electroadhesive composite gripper with proprioceptive and exteroceptive capabilities," *Mater. Des*. **156**, 586–587 (2018).
[11] M. Manti, T. Hassan, G. Passetti, N. D'Elia, C. Laschi and M. Cianchetti, "A bioinspired soft robotic gripper for adaptable and effective grasping," *Soft Robot.* **2**(3), 107–116 (2015).
[12] S. A. Suresh, D. L. Christensen, E. W. Hawkes and M. Cutkosky, "Surface and shape deposition manufacturing for the fabrication of a curved surface gripper," *J. Mech. Robot*. **7**(2), 021005 (2015).
[13] A. Pettersson, S. Davis, J. O. Gray, T. J. Dodd and T. Ohlsson, "Design of a magnetorheological robot gripper for handling of delicate food products with varying shapes," *J. Food Eng*. **98**(3), 332–338 (2010).
[14] W. Xu, H. Zhang, H. Yuanand B. Liang, "A compliant adaptive gripper and its intrinsic force sensing method," *IEEE Trans. Robot.* **37**(5), 1584–1603 (2021)..
[15] O. Pfaff, S. Simeonov, I. Cirovic and P. Stano, "Application of fin ray effect approach for production process automation," *Ann. DAAAM & Proc*. **22**(1), 1247–1249 (2011).
[16] FESTO, "Bionic Tripod 2.0." [Online]. *Available at:* https://www.festo.com.cn/net/en-cn_cn/SupportPortal/Downloads/146923. Accessed on: 2022.
[17] X. Shan and L. Birglen, "Modeling and analysis of soft robotic fingers using the Fin Ray effect," *Int. J. Robot. Res*. **39**(14), 1686–1705 (2020).
[18] C. Armanini, I. Hussain, M. Z. Iqbal, D. Gan, D. Prattichizzo and F. Renda, "Discrete cosserat approach for closed-chain soft robots: application to the fin-ray finger," *IEEE Trans. Robot.* **37**(6), 2083–2098 (2021).
[19] K. Elgeneidy, P. Lightbody, S. Pearson and G. Neumann, "Characterising 3D-Printed Soft Fin Ray Robotic Fingers with Layer Jamming Capability for Delicate Grasping," **In:** *2019 2nd IEEE International Conference on Soft Robotics (RoboSoft)* (2019) pp. 143–148.
[20] K. Elgeneidy, A. Fansa, I. Hussain and K. Goher, "Structural Optimization of Adaptive Soft Fin Ray Fingers with Variable Stiffening Capability," **In:** *3rd IEEE International Conference on Soft Robotics (RoboSoft)* (2020) pp. 779–784.
[21] L. Y. Lee, S. G. Nurzaman and C. P. Tan, "Design and Analysis of a Gripper with Interchangeable Soft Fingers for Ungrounded Mobile Robots," **In:** *2019 IEEE International Conference on Cybernetics and Intelligent Systems (CIS) and IEEE Conference on Robotics, Automation and Mechatronics (RAM)* (2019) pp. 221–226.
[22] C. I. Basson and G. Bright, "Geometric Conformity Study of a Fin Ray Gripper Utilizing Active Haptic Control," **In:** *2019 IEEE 15th 2019 IEEE 15th International Conference on Control and Automation (ICCA)* (2019) pp. 713–718.

[23] C. I. Basson, G. Bright and A. J. Walker, "Analysis of Flexible End-Effector for Geometric Conformity in Reconfigurable Assembly Systems: Testing Geometric Structure of Grasping Mechanism for Object Adaptability," **In:** *2017 Pattern Recognition Association of South Africa and Robotics and Mechatronics (PRASA-RobMech)* (2017) pp. 92–97.
[24] W. Crooks, G. Vukasin, M. O'Sullivan, W. Messner and C. Rogers, "Fin Ray effect inspired soft robotic gripper: from the robosoft grand challenge toward optimization," *Front. Robot. AI* **3**, 70 (2016).
[25] R. Chen, R. Song, Z. Zhang, L. Bai, F. Liu, P. Jiang and J. Guo, "Bio-inspired shape-adaptive soft robotic grippers augmented with electroadhesion functionality," *Soft Robot.* **6**(6), 701–712 (2019).
[26] F. Hannard, M. Mirkhalaf, A. Ameri and F. Barthelat, "Segmentations in fins enable large morphing amplitudes combined with high flexural stiffness for fish-inspired robotic materials," *Sci. Robot*. **6**(57), eabf9710 (2021).
[27] L. Wen, Z. Ren, V. Di Santo, K. Hu, T. Yuan, T. Wang and G. V. Lauder, "Understanding fish linear acceleration using an undulatory biorobotic model with soft fluidic elastomer actuated morphing median fins," *Soft Robot.* **5**(4), 375–388 (2018).
[28] M. H. Ali, A. Zhanabayev, S. Khamzhin and K. Mussin, "Biologically Inspired Gripper based on the Fin Ray Effect," **In:** *5th International Conference on Control, Automation and Robotics (ICCAR)* (2019) pp. 865–869.
[29] C. I. Basson, G. Bright and A. J. Walker, "Validating Object Conformity Through Geometric Considerations of Gripper Mechanisms," **In:** *2017 24th International Conference on Mechatronics and Machine Vision in Practice (M2VIP)* (2017) pp. 865–869.
[30] I. Hussain, M. Anwar, Z. Iqbal, R. Muthusamy, M. Malvezzi, L. Seneviratne and D. Prattichizzo, "Design and Prototype of Supernumerary Robotic Finger (SRF) Inspired by Fin Ray Effect for Patients Suffering from Sensorimotor Hand Impairment," **In:** *2019 2nd IEEE International Conference on Soft Robotics (RoboSoft)* (2019) pp. 398–403.
[31] Z. Deng and M. Li, "Learning optimal fin-Ray finger design for soft grasping," *Front. Robot. AI* **161** (2021).
[32] J. H. Shin, J. G. Park, D. I. Kim and H. S. Yoon, "A universal soft gripper with the optimized fin ray finger," *Int. J. Pr. Eng. Man-GT.* **8**(3), 889–899 (2021).
[33] D. D. Barrie, M. Pandya, H. Pandya, M. Hanheide and K. Elgeneidy, "A deep learning method for vision based force prediction of a soft fin ray gripper using simulation data," *Front. Robot. AI* **8**, 104 (2021).
[34] S. Alben, P. G. Madden and G. V. Lauder, "The mechanics of active fin-shape control in ray-finned fishes," *J. Roy. Soc. Interface* **4**(13), 243–256 (2007).

Cite this article: J. Yao, Y. Fang and L. Li (2023). "Research on effects of different internal structures on the grasping performance of Fin Ray soft grippers", Robotica **41**, 1762–1777. https://doi.org/10.1017/S0263574723000139